Letters on Materials 15 (4), 2025 pp. 344-349 www.lettersonmaterials.com

Received 13 August 2025; Accepted 1 November 2025
https://doi.org/10.48612/letters/2025-4-344-349 https://elibrary.ru/ynvcrg

Two-factor analysis of magnetic skyrmions stability in multilayer modified films

R. M. Vakhitov†, A. A. Akhmetova, M. A. Filippov, A. A. Khakimullina

†vakhitovrm@yahoo.com

Ufa University of Science and Technology, Ufa 450076, Russia

Abstract: The paper studies stable states of magnetic skyrmions arising in magnetically uniaxial nanomodified films, in which the Dzyaloshinskii–Moriya interaction takes place. The influence of defects of the "potential well" type on them is considered, in which the uniaxial anisotropy constant takes smaller but positive values, compared to the value of such in the main film array. The calculation was carried out by the method of micromagnetic modeling (using the open-access software package OOMMF), in which the film (of the Co/Pt type) was taken in the form of a disk, with a defect in its center. It is shown that, depending on the ratio of the Dzyaloshinskii–Moriya interaction parameter and the "potential well" depth, various types of magnetic vortex-like inhomogeneities are stabilized on the defect: $k\pi$-skyrmions (k=1, 2, 3), deformed skyrmion, incomplete skyrmion, etc. It has been established that the type of structure of inhomogeneities, their dimensions and threshold values of the "potential well" depth do not depend on the disk radius and are determined mainly by the value of the anisotropy constant outside the defect. At small values of the latter, magnetic vortices are stabilized in the center of the disk, which change their polarity when the defect is introduced (taken into account). The presence of two factors influencing the stability of vortex-like inhomogeneities in the films under study allows for more flexible control of their statics and dynamics, which creates certain prospects for their use in magnetic memory devices.

Keywords: nanoscale modified film, Dzyaloshinskii–Moriya interaction, uniaxial magnetic anisotropy, defect of the potential well type, magnetic skyrmion, magnetic vortex, polarization

Acknowledgements: *The authors are grateful for the financial support of the State assignment of Russian Federation for the implementation of scientific research by laboratories (no. 075-03-2024-123/1 15.02.2024).*

1. Introduction

Magnetic skyrmions are topologically stable vortex-like inhomogeneities that were discovered in MnSi films more than 15 years ago [1]. Since then, interest in them has grown exponentially among various research groups, which has resulted in the emergence of a separate area of research in magnetism on such structures, called skyrmions [2]. Such attention to skyrmions was primarily due to a number of unique properties discovered in them (topological protection, nanosize, high mobility, controlled response to external influences, etc.), which can find application in various spintronic devices, including artificial neural networks [3] and new-generation magnetic memory [4]. The main factor stabilizing the structure of magnetic skyrmions in films related to chiral magnets [5] is the presence of the Dzyaloshinskii-Moriya interaction (DMI), which can manifest itself in materials such as MnSi as a bulk interaction [6], and in multilayer films as an interfacial DMI [7].

At the same time, as studies have shown [8–10], there is another factor that can also lead to the stabilization of skyrmions. This is the presence of "potential well" type defects in films, which can be artificially obtained by irradiating the sample surface with He^+ or Ca^+ ions [11]. A uniaxial film modified in this way will contain areas with altered values of material parameters, and, in particular, with a reduced value of uniaxial anisotropy (a "potential well" type defect). In this case, under certain conditions, magnetic skyrmions can originate on the defects, the stability of which is primarily determined by the characteristics of the defect, its size and the depth of the "potential well" [12–14]. However, if the film is multilayered like Co/Pt [15], then in this case, due to the violation of inversion symmetry arising at the interface between two phases (magnetic–non-magnetic), it is necessary to take into account the effect on the stability of skyrmions and the presence of interphase DMI. Such an approach was implemented in [16], in which the effect of both factors on the stability of skyrmions was considered, and it was assumed that the easy-plane magnetic anisotropy occurs at the defect.

In this paper, the effect of a similar defect of the "potential well" type is considered, however, in the defect area, the magnetic anisotropy value is considered positive, but smaller in value compared to the rest of the film. This will simplify the synthesis of such nanomodified films, and facilitate their possible potential application in spintronic devices of magnetic memory based on skyrmions.

2. Model and computational methods

The films under consideration were studied using the micromagnetic modeling method in the open-access software packages OOMMF [17] and Ubermag [18]. The film is considered in the form of a disk of radius R. A defect of radius R_0 is located in the center of the disk, while their axial axes of symmetry coincide and are perpendicular to the plane of the film. The exchange interaction (determined by the constant A), DMI (D), demagnetizing fields caused by the finiteness of the disk (saturation magnetization M_s) and the presence of perpendicular magnetic anisotropy (PMA), the easy axis of which is directed perpendicular to the plane of the film are taken into account in the modeling. The presence of a defect in the sample is taken as a dependence of the PMA constant on the radial variable r according to the formula:

$$K_u = \begin{cases} K_{u1}, & r > R_0 \\ K_{u2}, & 0 \le r \le R_0 \end{cases}, \qquad (1)$$

where K_{u1} is the value of magnetic anisotropy outside the defect, and K_{u2} is on the defect ($K_{u1} > K_{u2}$).

At the initial stage, a search was carried out for the range of material parameter values, in which stable magnetic vortex-like inhomogeneities would be observed. For this purpose, the following sets of parameters specified during modeling were considered: $R = 75$ nm, $h = 1$ nm, $K_{u1} = (0.1 \div 2.0) \cdot 10^6$ J/m^3, $A = 1.5 \cdot 10^{-12}$ J/m, $M_s = 4 \cdot 10^5$ A/m, $D = (0.5 \div 4.0) \cdot 10^{-3}$ J/m^2. These material parameters correspond to multilayer films of the Co/Pt type Co/Pt [19–21]. In the center of the disk, a region with magnetization opposite to the direction of magnetization of the rest of the disk and the anisotropy axis was initially specified.

3. Results and discussion

During the calculations, a stability diagram of various spin textures was obtained, shown in Fig. 1a. It follows from it that the region of existence of Néel type skyrmions increases with increasing DMI constant, but at higher anisotropy values the disk becomes uniformly magnetized. However, at lower K_{u1}, structures other than π-skyrmions are stabilized on the disk: incomplete skyrmions [22], 2π- and 3π-skyrmions [2] (Fig. 2a–c)), deformed skyrmions of various types.

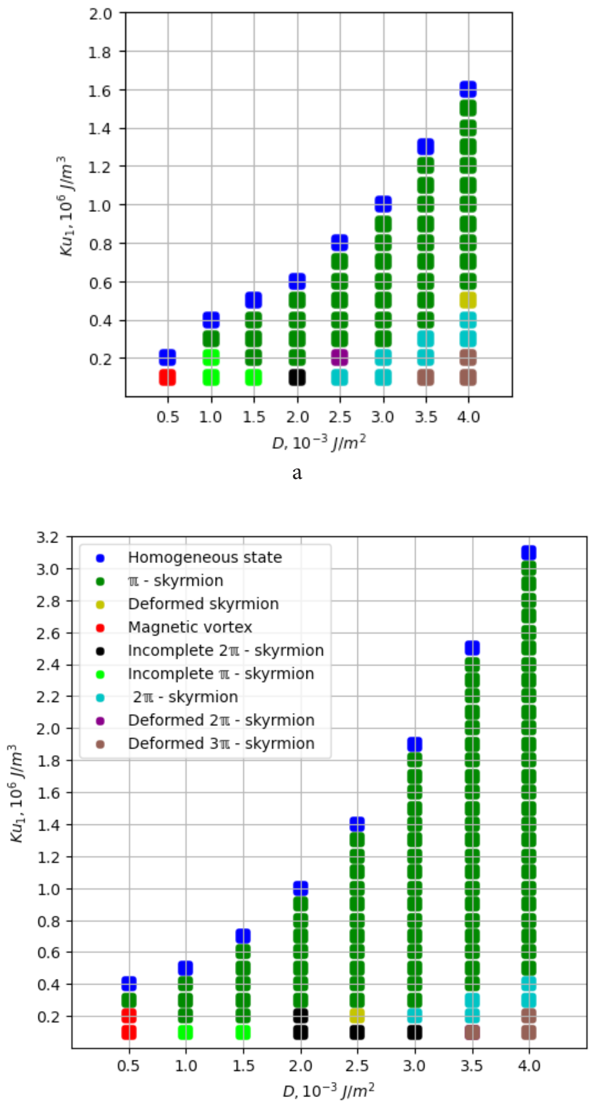

Fig. 1. (Color online) Stability diagram of magnetic skyrmions in the absence of a defect (a) and in the presence of a defect (b).

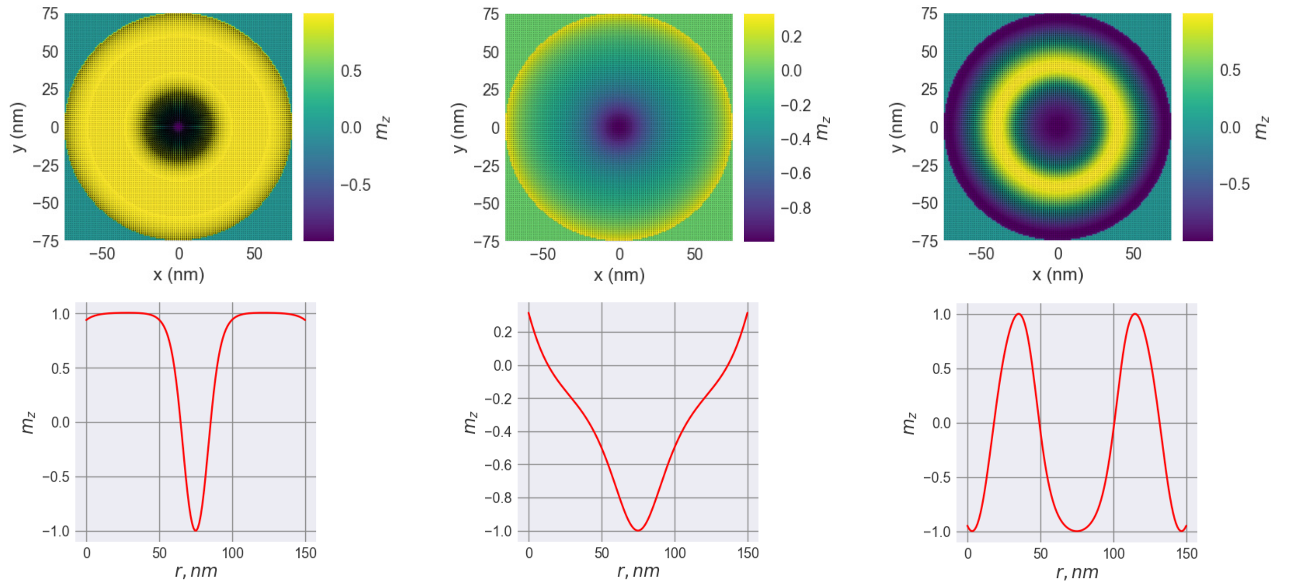

a b c

Fig. 2. (Color online) Some types of magnetic structures and their magnetization distribution: π-skyrmion (a), incomplete π-skyrmion (b), 2π-skyrmion (c).

Deformed magnetic skyrmions are skyrmions whose shapes lack axial symmetry but have rotational symmetry axes of 4th, 6th, and so on, which is most likely due to the choice of model shape. These structures pass into the skyrmion state with increasing K_{u1}. In this case, 2π and 3π-skyrmions begin to appear only for values of $D > 2.5\cdot10^{-3}$ J/m². To study the effect of the presence of defects, a cylindrical defect in the center of the disk was added to the calculation model, on which the value of magnetic anisotropy decreased by 2 times, i.e. $K_{u2} = 0.5K_{u1}$. All other material parameters remained the same. The stability diagram of magnetic structures in the presence of such a defect is shown in Fig. 1b. It shows a significant expansion of the skyrmion stabilization region. At large D, this region expands almost 2 times. However, this effect is manifested only for π-skyrmions. More complex spin structures (2π- and 3π-skyrmions) also remain stable only at small K_{u1}. Based on this, we can conclude that the presence of a defect has a positive effect on the stability of π-skyrmions, which in this case expands significantly.

For a more detailed examination of the defect influence and the transition from the homogeneous disk state to the skyrmion state, two points were selected on the stability diagram in the absence of a defect (Fig. 1a), at which the skyrmion does not stabilize under the given conditions: $D = 1.0\cdot10^{-3}$ J/m² and $K_{u1} = (0.4 \text{ and } 0.6)\cdot10^{6}$ J/m³. A "potential well" type defect with a radius of $R_0 = (10, 20, 30)$ nm is added in the disk center, at which K_{u2} gradually decreases to 0 with a step of $0.1\cdot10^{6}$ J/m³. To additionally examine the influence of magnetostatic interaction and to be able to numerically obtain more complex vortex-like textures, two disk radii with $R = 75$ and 150 nm were selected. At $K_{u1} = 0.4\cdot10^{6}$ J/m³ and $R_0 = 30$ nm, the skyrmion on the disk is stabilized at $K_{u2} = 0.25\cdot10^{6}$ J/m³ for both film sizes. At $K_{u1} = 0.6\cdot10^{6}$ J/m³ and $R_0 = 30$ nm, the skyrmion becomes stable only at $K_{u2} = 0.1\cdot10^{6}$ J/m³. In this case, as the "potential well" depth increases, the skyrmion size increases and approaches the defect size (Fig. 3). Note that the skyrmion size is determined only by the ratio of the magnetic anisotropy values on the defect and in the rest of the disk and does not depend on the disk size itself. The maximum radius of the skyrmion R_V is achieved at $K_{u2} = 0$ J/m³.

In addition, the film energy values were analyzed when skyrmions appeared on the defect. The nature of the change in the total disk energy and the interaction energies included in the model also depends only on K_{u1}. Figure 4 shows the energy change graphs for a disk with $R = 75$ nm for cases with $K_{u1} = (0.4 \text{ and } 0.6)\cdot10^{6}$ J/m³.

In both cases, when the threshold value K_{u2} is reached, at which a skyrmion occurs, first there is a jump in the total disk energy, then it begins to decrease to values below the energy of the homogeneous state. This indicates the stability of skyrmions on the defects introduced into the disk model. The energy of the PMA begins to decrease due to the appearance of a region with a reduced anisotropy value. The energy of the exchange interaction increases due to the violation of the homogeneous state of magnetization. The modulus of the DMI energy also increases due to the appearance of a magnetization gradient during the formation of a skyrmion. The energy of the magnetostatic interaction, on the contrary, decreases. Due to the appearance of a skyrmion, on which the magnetic flux is closed, a decrease in the energy of the magnetostatic fields occurs. For a disk of a larger size, the nature of the energy change during the transition coincides with that described above.

To verify the fact of contraction of the skyrmion sizes to the defect sizes, we simulated a film with similar defects

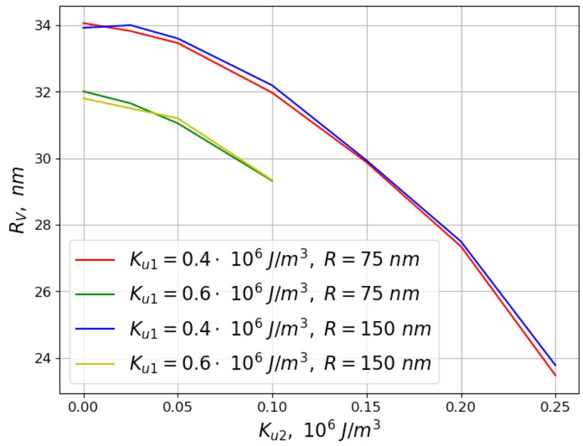

Fig. 3. (Color online) Graph of the dependence of the skyrmion radius R_V on K_{u2} at $R_0 = 30$ nm.

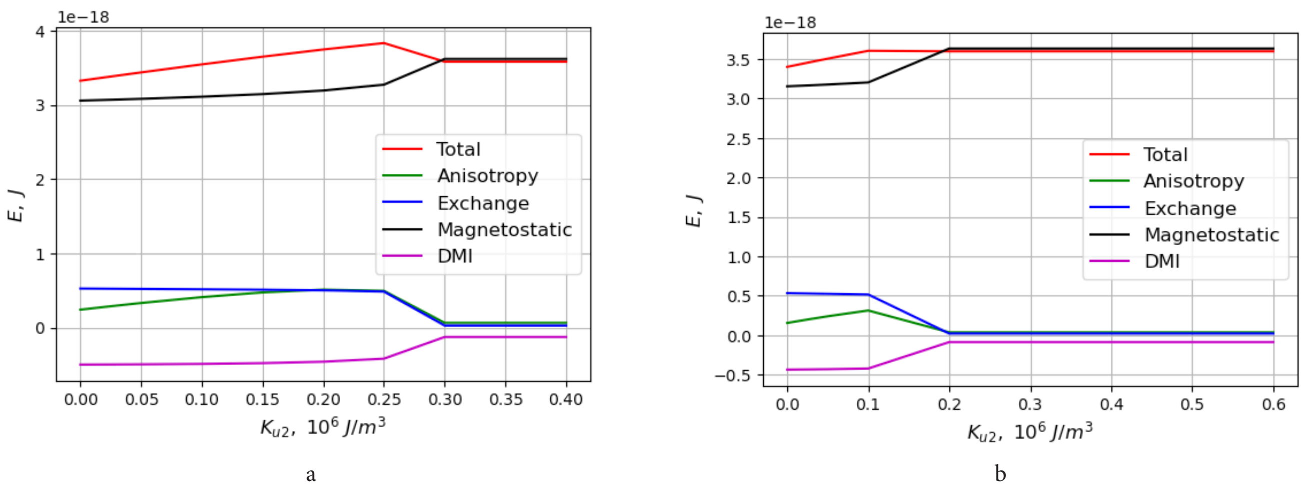

Fig. 4. (Color online) Disk energy at $R = 75$ nm depending on K_{u2}: $K_{u1} = 0.4\cdot10^{6}$ J/m³ (a) $K_{u1} = 0.6\cdot10^{6}$ J/m³ (b).

but with smaller radii: 20 and 10 nm. At $R_0 = 20$ nm, the stabilization process and threshold values for the appearance of the skyrmion state K_{u2} coincide with the cases considered above at $R_0 = 30$ nm. But the radius of stable skyrmions changes (Fig. 5), its value R_V now tends to 20 nm. In this case, the defect radius also depends only on the ratio of the K_{u1} and K_{u2} values. If we reduce the defect radius R_0 to 10 nm, the skyrmions stabilize only at $K_{u1} = 0.4 \cdot 10^6$ J/m³ with a threshold value of $K_{u2} = 0.1 \cdot 10^6$ J/m³. For both disk sizes, $R_V \approx 10$ nm. Thus, the fact of contraction of the skyrmion dimensions to the defect dimensions with decreasing K_{u2} takes place.

Subsequently, a more detailed study of the conditions for the existence of vortex-like inhomogeneities was carried out with a lower DMI coefficient $D = 0.5 \cdot 10^{-3}$ J/m² (Table 1).

According to the obtained results (Table 1), we see that the type of structure, its dimensions, and the threshold value of the appearance of the skyrmion K_{u2} are also determined only by the value of K_{u1} and do not depend on R. Minor changes are observed at small K_{u1}. But even at a smaller value of DMI, in the presence of a defect, it is possible to obtain stable magnetic skyrmions, although the region of their existence decreases. Particular attention was paid to the results with films at $K_{u1} = 0.1 \cdot 10^6$ J/m³. In this case, magnetic vortices are stabilized in the center of the disk, regardless of the depth of the potential well. In this case, the rotation of the magnetization vector in the film occurs according to the Bloch and Néel laws, in contrast to the cases with $D = 1.0 \cdot 10^{-3}$ J/m², when only Néel skyrmions are stable. This can be explained by a decrease in the DMI parameter, which is demonstrated in Fig. 6, where the directions of the magnetization vectors of the vortex (Fig. 6a) and skyrmion (Fig. 6b) are schematically shown for the same film size and defect. Here it should be noted that in Fig. 6a there is in fact a more complex structure, in which at the periphery ($r \to R$)

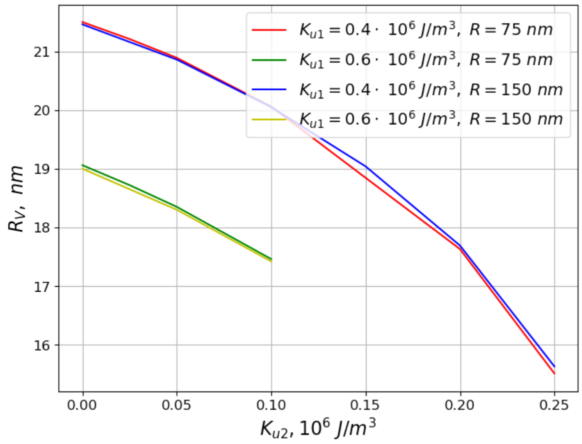

Fig. 5. (Color online) Graph of the dependence of the skyrmion radius R_V on K_{u2} at $R_0 = 20$ nm.

Table 1. Results of modeling stable vortex-like structures at $D = 0.5 \cdot 10^{-3}$ J/m² and $R_0 = 30$ nm.

R, nm	K_{u1}, J/m³	Threshold value, K_{u2}, J/m³	Vortex-like structure	Skyrmion radius R_V, nm
75	$0.4 \cdot 10^6$	$0.15 \cdot 10^6$	Skyrmion	24
150	$0.4 \cdot 10^6$	$0.15 \cdot 10^6$	Skyrmion	24
75	$0.3 \cdot 10^6$	$0.2 \cdot 10^6$	Skyrmion	22
150	$0.3 \cdot 10^6$	$0.2 \cdot 10^6$	Skyrmion	23
75	$0.2 \cdot 10^6$	$0.05 \cdot 10^6$	Incomplete skyrmion	-
150	$0.2 \cdot 10^6$	For all values K_{u2}	Incomplete skyrmion	-
75	$0.1 \cdot 10^6$	For all values K_{u2}	Vortex	-
150	$0.1 \cdot 10^6$	For all values K_{u2}	Vortex	-

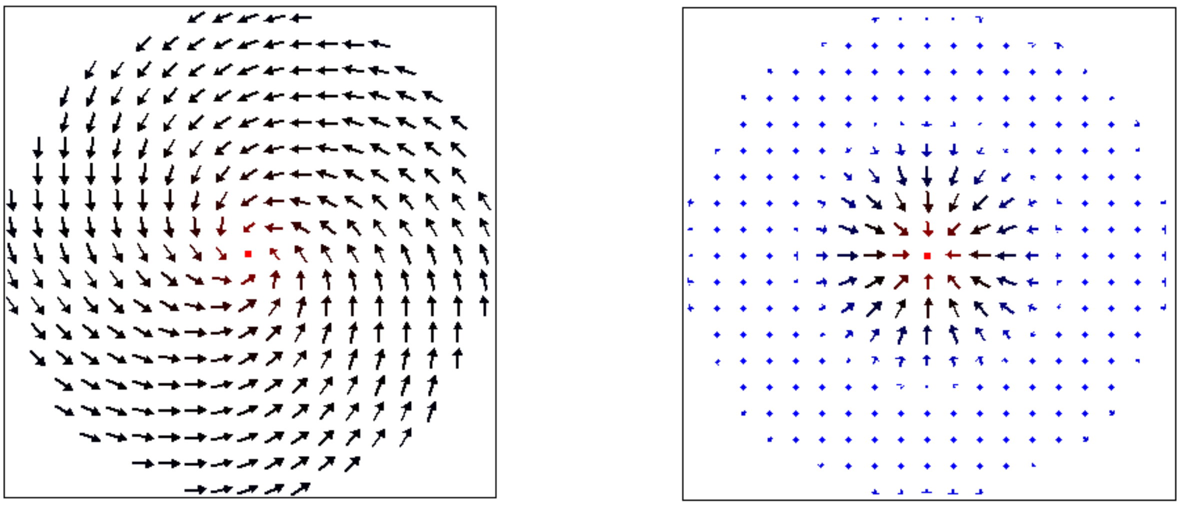

a b

Fig. 6. (Color online) Magnetic vortex at $D = 0.5 \cdot 10^{-3}$ J/m², $K_{u1} = 0.1 \cdot 10^6$ J/m³, $K_{u2} = 0$, $R = 75$ nm (a); magnetic skyrmion at $D = 1.0 \cdot 10^{-3}$ J/m², $K_{u1} = 0.4 \cdot 10^6$ J/m³, $K_{u2} = 0$, $R = 75$ nm; red color — the magnetization vector is directed perpendicular to the film plane and away from the observer, blue — perpendicular to the film plane and towards the observer, black — in the film plane.

the rotation of the magnetization vector **m** occurs purely according to the Bloch law, and as one approaches the center of the disk, a Neel component appears in the magnetization distribution (although it is noticeably smaller in magnitude than the Bloch one). In the case of an increase in the film size to R=150 nm, the introduction of a defect causes a switch in the polarity of the vortex to the opposite (Fig. 7): in the absence of a defect, the polarity is equal to 1, and when a defect with $K_{u2}=0$ is introduced, the polarity becomes equal to −1. In addition, the vortex profile narrows in the defect area.

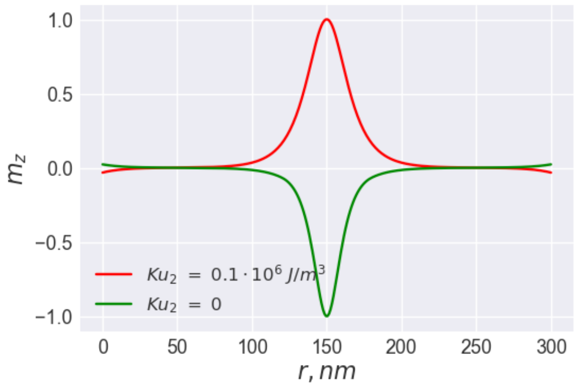

Fig. 7. (Color online) Graph of the distribution of vortex magnetization at R=150 nm and $K_{u1}=0.1\cdot10^6$ J/m^3.

4. Conclusions

In the presented work, the influence of the presence of a defect of the "potential well" type in a magnetically uniaxial multilayer disk-shaped film on the region of existence of single magnetic skyrmions in the disk-shaped film was studied. The simulation results showed that in the presence of a defect, the range of material parameters at which skyrmions are stabilized expands. In this case, the structure and dimensions of the skyrmion formed on the defect are determined only by the dimensions of the defect and its depth (K_{u2}), and do not depend on the dimensions of the disk itself. The dimensions of the disk begin to have an effect only at small K_{u1}. In addition, it was shown that by varying the material parameters, but without changing the dimensions of the film, it is possible to obtain different types of vortex-like inhomogeneities (incomplete skyrmion, magnetic vortex, 2π- and 3π- skyrmions). In the case when magnetic vortices are stabilized, a switch in the polarity of the vortex was detected when a defect appeared in the film. From the results presented, it follows that the presence of two factors on the stability of magnetic skyrmions in the films under study allows for more flexible control of them, which has practical significance for their possible use in new-generation information recording and reading devices.

References

1. S. Mühlbauer, B. Binz, F. Jonietz, C. Pfleiderer, A. Rosch, A. Neubauer, R. Georgii, P. Böni, Skyrmion Lattice in a Chiral Magnet, Science 323 (2009) 915–919.
2. K. Everschor-Sitte, J. Masell, R.M. Reeve, M. Kläui, Perspective: Magnetic skyrmions — Overview of recent progress in an active research field, J. Appl. Phys. 124 (2018) 240901.
3. O. Lee, R. Msiska, M.A. Brems, M. Kläui, H. Kurebayashi, K. Everschor-Sitte, Perspective on unconventional computing using magnetic skyrmions, Appl. Phys. Lett. 122 (2023) 260501.
4. H. Zhang, Y. Zhang, Z. Hou, M. Qin, X. Gao, J. Liu, Magnetic skyrmions: materials, manipulation, detection, and applications in spintronic devices, Mater. Futures 2 (2023) 032201.
5. A.N. Bogdanov, C. Panagopoulos, The emergence of magnetic skyrmions, Physics Today 73 (2020) 44–49.
6. K.K. Mishra, A.H. Lone, S. Srinivasan, H. Fariborzi, G. Setti, Magnetic skyrmion: from fundamental physics to pioneering applications, Appl. Phys. Rev. 12 (2025) 011315.
7. A. Fert, N. Reyren, V. Cros, Magnetic skyrmions: advances in physics and potential applications, Nat. Rev. Mater. 2 (2017) 17031.
8. D. Navas, R.V. Verba, A. Hierro-Rodriguez, S.A. Bunyaev, X. Zhou, A.O. Adeyeye, O.V. Dobrovolskiy, B.A. Ivanov, K.Y. Guslienko, G.N. Kakazei, Route to form skyrmions in soft magnetic films, APL Materials 7 (2019) 081114.
9. A.S. Samardak, A.G. Kolesnikov, A.V. Davydenko, M.E. Steblii, A.V. Ognev, Topologically Nontrivial Spin Textures in Thin Magnetic Films, Phys. Metals Metallogr. 123 (2022) 238–260.
10. L.G. Korzunin, I.M. Izmozherov, Numerical Simulation of the Influence of Inhomogeneities on the Properties of Magnetization Nanostructures, Phys. Metals Metallogr. 122 (2021) 169–196.
11. M.V. Sapozhnikov, S.N. Vdovichev, O.L. Ermolaeva, N.S. Gusev, A.A. Fraerman, S.A. Gusev, Yu.V. Petrov, Artificial dense lattice of magnetic bubbles, Appl. Phys. Lett. 109 (2016) 042406.
12. R.M. Vakhitov, A.A. Akhmetova, R.V. Solonetskii, Vortex-like Structures at the Defects of Uniaxial Films, Phys. Solid State 61 (2019) 319–325.
13. R.M. Vakhitov, R.V. Solonetsky, A.A. Akhmetova, Stable states of vortex-like magnetic formations in inhomogeneous magnetically uniaxial films and their behavior in a longitudinal magnetic field, J. Appl. Phys. 128 (2020) 153904.
14. R.M. Vakhitov, R.V. Solonetsky, A.A. Akhmetova, M.A. Filippov, Behavior of Vortex-Like Inhomogeneities Originating in Magnetic Films with Modulated Uniaxial Anisotropy in a Planar Magnetic Field, Symmetry 14 (2022) 612.
15. C. Moreau-Luchaire, C. Moutafis, N. Reyren, J. Sampaio, C.A.F. Vaz, N. Van Horne, K. Bouzehouane, K. Garcia, C. Deranlot, P. Warnicke, P. Wohlhüter, J.-M. George, M. Weigand, J. Raabe, V. Cros, A. Fert, Additive interfacial chiral interaction in multilayers for stabilization of small individual skyrmions at room temperature, Nature Nanotech. 11 (2016) 444–448.
16. R.M. Vakhitov, A.A. Akhmetova, M.A. Filippov, Possible structures of skyrmion states in chiral ferromagnetic films

with spatially modulated uniaxial anisotropy, J. Phys.: Condens. Matter. 37 (2025) 055802.
17. M. Donahue, D.G. Porter, OOMMF User's Guide, Version 1.0, Technical Report, NIST Interagency Report No. 6376 (National Institute of Standard and Technology, Gaithersburg, MD, 1999).
18. M. Beg, M. Lang, H. Fangohr, Ubermag: Toward More Effective Micromagnetic Workflows, IEEE Trans. Magn. 58 (2022) 1–5.
19. J. Sampaio, V. Cros, S. Rohart, A. Thiaville, A. Fert, Nucleation, stability and current-induced motion of isolated magnetic skyrmions in nanostructures, Nature Nanotech. 8 (2013) 839–844.
20. Y. Zhou, M. Ezawa, A reversible conversion between a skyrmion and a domain-wall pair in a junction geometry, Nat Commun. 5 (2014) 4652.
21. Y. Zhou, E. Iacocca, A. A. Awad, R. K. Dumas, F. C. Zhang, H. B. Braun, J. Åkerman, Dynamically stabilized magnetic skyrmions, Nat Commun. 6 (2015) 8193.
22. T. B. Winkler, K. Litzius, A. De Lucia, M. Weißenhofer, H. Fangohr, M. Kläui, Skyrmion States in Disk Geometry, Phys. Rev. Applied 16 (2021) 044014.